Mesoporous Materials

DOI: 10.1002/anie.200503301

Tuning the Structure and Orientation of Hexagonally Ordered Mesoporous Channels in Anodic Alumina Membrane Hosts: A 2D Small-Angle X-ray Scattering Study**

*Barbara Platschek, Nikolay Petkov, and Thomas Bein**

Periodic mesoporous materials have attracted considerable attention during the last decade because of their promising applications as catalyst supports and nanoreactors, or as hosts for nanostructured materials with appealing optoelectronic properties.[1,2] Many of these applications will benefit from arrangements of preferentially aligned, ordered arrays of certain mesostructures. The evaporation-induced self-assembly (EISA) method has been established as an efficient process for the preparation of thin films with mono-oriented mesostructured domains.[3,4] However, the most frequently obtained films display hexagonally ordered channels that are aligned parallel to the surface of the substrate.[5]

Recently, the synthesis of mesoporous materials within the regular, larger channels of anodic alumina membranes (AAMs) has been explored, with the aim of attaining greater control over the morphology of the mesoporous system.[6] A first approach, through a sol–gel synthesis route using the triblock copolymer poly(ethylene oxide)$_{100}$-b-poly(propylene oxide)$_{65}$-b-poly(ethylene oxide)$_{100}$ ($PEO_{100}PPO_{65}PEO_{100}$ or Pluronic F-127) as a structure-directing agent, resulted in 2D hexagonal mesostructures with two different orientations that were found to coexist at different ratios depending on the concentration of the surfactant.[7] In one case, the long axes of the mesopores were aligned with the long axes of the AAM channels (columnar orientation). In another case, a circular orientation of the mesostructure was observed. Similar (free-standing) unusual mesophase structures are known to exist in cetyltrimethylammonium bromide (CTAB)-templated materials prepared by solvothermal methods and have been named "circulites" or circular crystals.[8,9]

The efficient EISA method can also be used to prepare AAM mesoporous composite materials by applying coating solutions that are typically used for the deposition of mesoporous silica films. When using cationic CTAB as a template, partially ordered mesoporous materials with aligned, columnar mesopores only in the vicinity of the alumina walls were obtained that showed promising behavior as molecular separators.[10] Use of the triblock copolymer $PEO_{20}PPO_{70}PEO_{20}$ (Pluronic123 or P123) as a template resulted in striking mesostructures with concentric or helical mesopores and single chains of spherical mesopores, depending on the confinement conditions imposed by alumina nanochannels with diameters of less than 100 nm.[11] In contrast, columnar mesopores were reported when the same template (P123) was used in the sol–gel approach in larger Anopore channels.[12] However, when a slightly different protocol at the same surfactant/silica ratio was used in the sol–gel synthesis route, hexagonal mesophases with mixed orientations resulted.[13] The presence of water vapor in the ageing process was investigated in a related study using the P123 template.[14,15] In this case, the circular orientation was favored over the columnar one at higher water pressure; this selectivity was attributed to the increased rate of gelation. Multiple mesoporous silica phases have also been included in AAM channels through sequential loading techniques.[16]

From the studies discussed above, it is clear that subtle changes in stoichiometry and reaction conditions can lead to striking changes in the order and morphology of the mesopores. With an aim to better understand the mechanism and the ability to tune these intriguing structures at will, we present herein a combined 2D small-angle X-ray scattering (SAXS) and transmission electron microscopy (TEM) study, which shows that highly ordered hexagonal mesoporous structures with adjustable orientation can be formed with the templates CTAB, P123, and decaethylene glycol hexadecyl ether (Brij56) under the conditions of the EISA method. We demonstrate that when using the ionic surfactant CTAB, the hexagonally structured mesopores are solely oriented along the AAM channels. With the non-ionic surfactants P123 or Brij56, it was possible to control the formation of either orientation (circular or columnar) by tuning the silica-to-surfactant ratio of the initial synthetic mixtures as well as the humidity level during the EISA process.

The method used here for the self-assembly of the ordered silica/surfactant nanocomposites in the channels of the anodic alumina membranes is depicted in Figure 1. The AAMs used in this study showed almost hexagonal packing of vertical pores, with diameters in the range of 120–200 nm, through the entire thickness of the membrane (Figure 2a). The synthetic mixtures containing the silica precursor and either CTAB, P123, or Brij56 as structure-directing agents were introduced into the pores of the AAM by soaking the membranes at room temperature in a flat pool of liquid. As a result of evaporation of the solvent, which progressively increases the concentration of the surfactant and other nonvolatile components of the synthetic mixtures, the self-assembly process is driven towards the formation of micelles and the condensation of silica, followed by a disorder-to-order transition to provide the final, extended mesophase structure.

Figure 2a and b show side-view scanning electron microscopy (SEM) images of the AAM before and after loading with P123-templated mesoporous silica, respectively. As expected, pure AAMs show well-aligned, almost regularly arranged nanochannels (Figure 2a). After the assembly of the mesoporous silica structures using CTAB or P123 as structure-directing agents, well-shaped nanoscopic filaments that

[*] B. Platschek, Dr. N. Petkov, Prof. Dr. T. Bein
Department of Chemistry and Biochemistry
University of Munich (LMU)
Butenandtstrasse 11, 81377 Munich (Germany)
Fax: (+49) 89-2180-77622
E-mail: bein@lmu.de

[**] This work was supported by the SFB486 of the German Research Foundation (DFG).

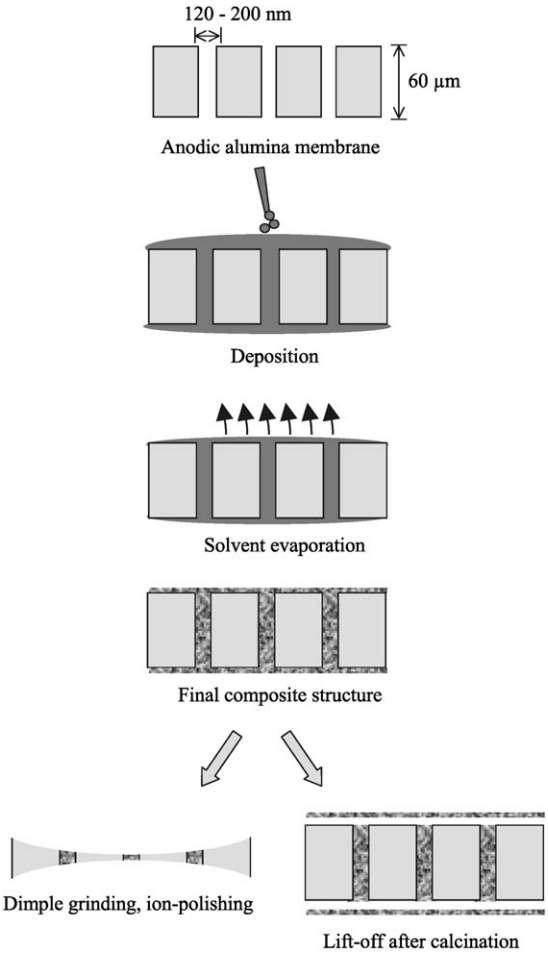

Figure 1. Schematic representation of the synthetic route to obtain mesostructured silica–surfactant nanocomposites in the AAMs.

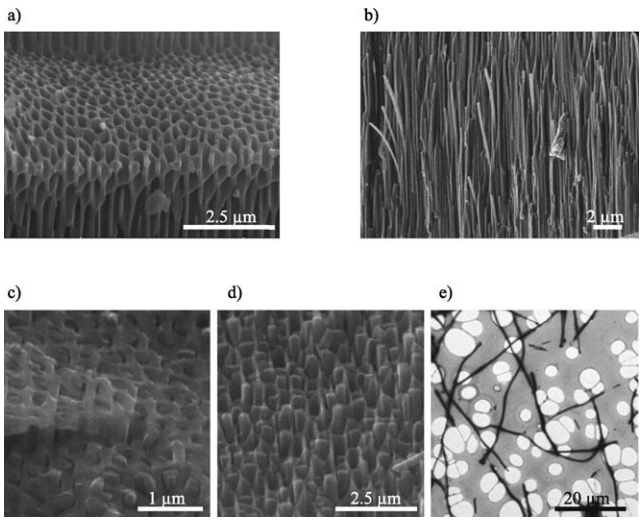

Figure 2. a, b) Side-view SEM images of sample D1 (with P123) showing the morphology of the AAMs before (a) and after (b) inclusion of mesoporous silica. c, d) SEM images of the silica filaments encapsulated within pores of AAMs, templated with CTAB (c) and P123 (d). e) TEM image of the isolated silica filaments imaged on a holey carbon grid (sample CTAB1).

protrude from the openings of the AAM channels were observed (Figure 2c, d). Figure 2b depicts the uniformity and continuity of the as-deposited nanostructures, viewed normal to the direction of the channel of the membrane, while Figure 2e shows the isolated mesoporous 1D nanofibers obtained by dissolution of the AAM matrix in phosphoric acid. Energy-dispersive X-ray (EDX) measurements taken along the whole thickness of the membrane showed similar Al/Si atomic ratios, demonstrating the continuous and homogeneous filling of the membrane with the silica–surfactant nanocomposites.

The geometry of the SAXS experiments, performed close to the grazing angle, and the proposed mesophase structures are shown in Figure 3. Both out-of-plane and in-plane

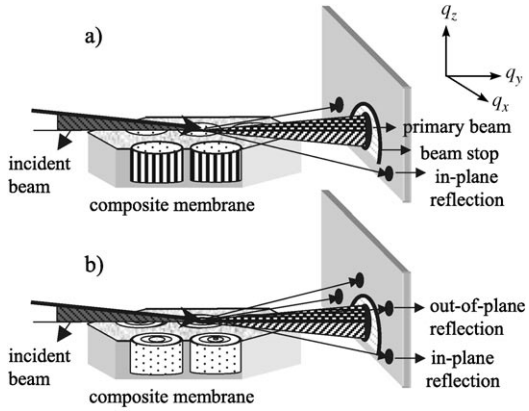

Figure 3. Geometry of the grazing incidence (GI)-SAXS experiment for the mesophase structures with a) hexagonally ordered mesopores fully aligned along the channels of the AAMs (columnar orientation) and b) circular mesopores with local hexagonal order parallel to the surface of the AAMs.

diffracted beams were recorded simultaneously. Full alignment of the mesoporous channels in the direction perpendicular to the membrane surface (parallel to the channels of the AAMs) will result in only two reflections in the direction of the q_x vector and the absence of out-of-plane reflections (Figure 3a). This distinct case was observed for the two CTAB-templated samples that were prepared at different concentrations of surfactant (see Figure 4 and Experimental Section). The indexing of the diffraction spots is given in Figure 4a. These highly structured mesophases are directly observed in the representative plan-view TEM images shown in Figure 5a. For the sample CTAB2, almost all of the pores of the alumina membrane (about 90%) were filled with fully mesostructured material. The power spectrum (inset in Figure 5a) calculated from the corresponding TEM image showed a well-ordered hexagonal mesophase structure with a d spacing of about 4.5 nm, which corresponds to the spacing observed for CTAB-templated mesoporous powders (e.g. MCM-41-type materials).[17] We observe that with a decrease in the concentration of the surfactant in the deposition mixtures (sample CTAB1, Figure 4a), the intensity of the diffraction spots in the SAXS patterns also decreases (Table 1). This behavior is due to the decreased density of the ordered mesostructured domains in the alumina matrix.

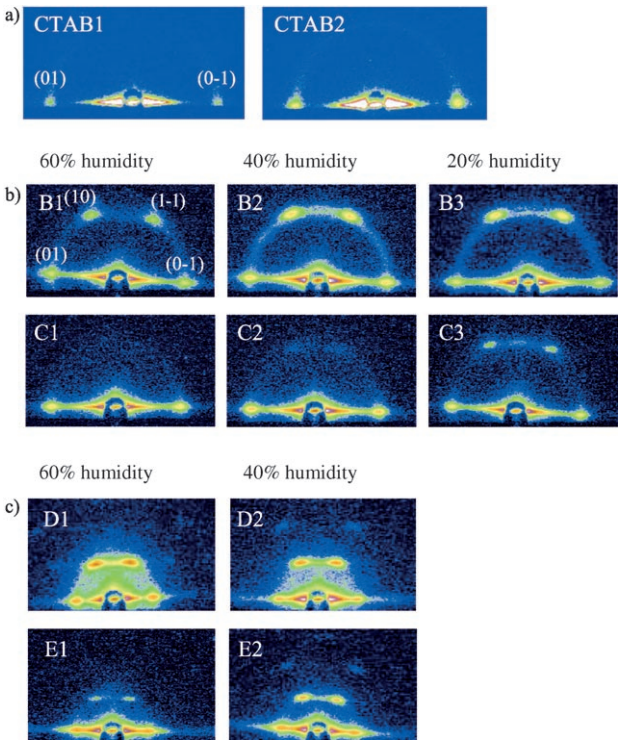

Figure 4. GI-SAXS patterns of the samples: a) CTAB1 and CTAB2 (templated with different concentrations of CTAB), b) B1–B3 and C1–C3 (templated with Brij56 but at different surfactant concentrations (B, C) and humidities (1–3)), and c) D1, D2, E1, and E2 (templated with P123 but at different surfactant concentrations (D, E) and humidities (1, 2)). All images are shown with the same spatial and intensity scale. See text and Experimental Section for details. For the circular structure, a system of rings is found in reciprocal space.[8] Indexation is given as for the normal hexagonal lattice.

Table 1: Summary of SAXS data of CTAB-templated mesoporous channel systems.

Sample	Surfactant/silica molar ratio	Diffraction spots detected	Relative intensity[a]	*d* spacing[b]
CTAB1	0.18	(01); (0-1)	0.14	4.5
CTAB2	0.26	(01); (0-1)	0.19	4.3

[a] The intensity of the reflections was normalized to the intensity of the primary beam after the semitransparent beam stop. [b] The *d* spacings were calculated from the position of the diffraction spots according to $q = 2\pi/d$.

The corresponding TEM images from this sample show that almost 30% of the alumina pores are either empty or show inferior hexagonal order. The results suggest that the ordering process (formation of the lyotropic liquid-crystalline mesophase) can be directly controlled by varying the concentrations of surfactant in the deposition mixtures.

The second mesophase configuration (circular mesopores) that was studied here by using P123 or Brij56 as structure-directing agents is schematically shown in Figure 3b. With these samples, four well-resolved diffraction spots from both out-of-plane and in-plane reflections were recorded (see Figure 4b for indexing). This diffraction pattern can be identified as one that arises from the local hexagonal

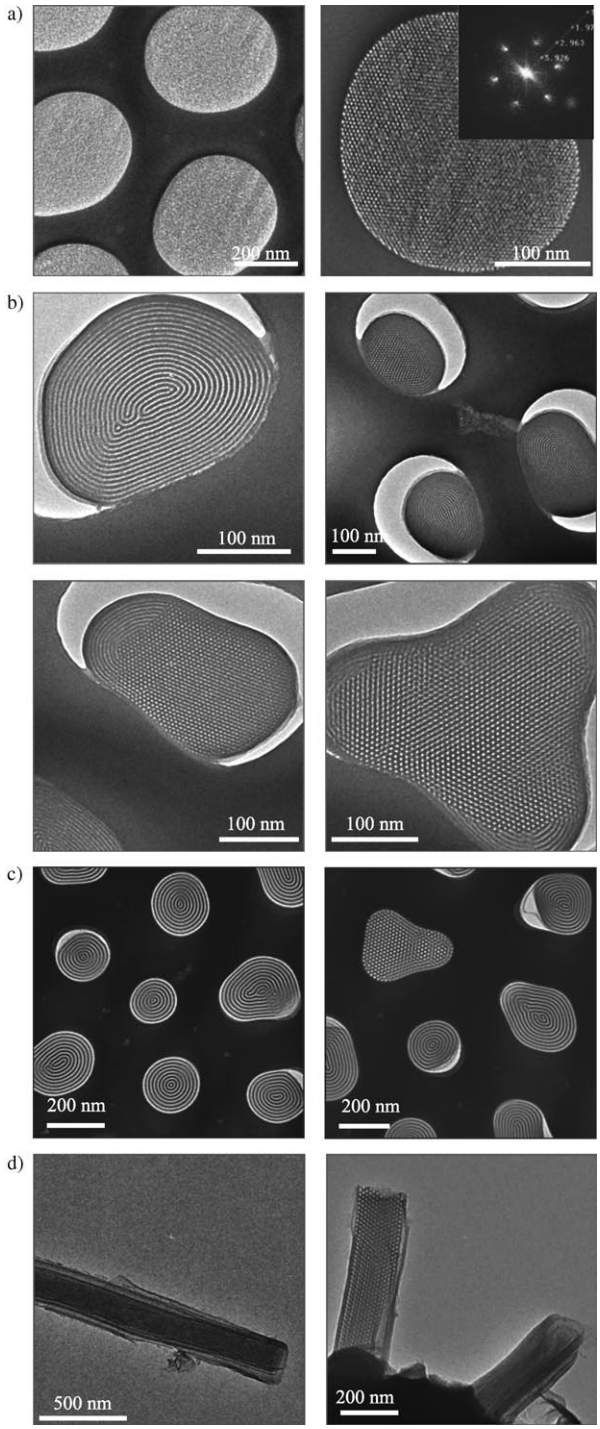

Figure 5. a)–c) Plan-view TEM images of samples a) CTAB2 showing the columnar oriented hexagonal mesostructure (insert: 2D power spectrum), b) B1 (templated with Brij56 at 60% humidity) with approximately equal distribution of columnar and circular mesophases, showing AAM pores with columnar or circular orientation as well as an AAM pore with a hybrid structure, and c) D1 (templated with P123 at 60% humidity; predominantly circular orientation). d) Cross-section TEM image of sample E1 (templated with P123 at 60% humidity; predominantly columnar orientation) showing mesoporous fibers protruding from the AAM channels at a site of fracture.

arrangement of mesopores with the (100) lattice plane (i.e. the close packing of mesopore channels) parallel to the curved AAM channel surface (the two missing diffraction spots, below the membrane surface, are shadowed by the beam stop). To record plan-view TEM images the structure was imaged in the direction perpendicular to the membrane surface, and circular, concentric mesophase channels as well as some columnar channels were observed (see Figure 5b and c for the Brij56- and P123-templated structures, respectively).

We observed that the mesophase structure of the AAM-embedded P123- and Brij56-templated materials (columnar or circular pore orientation) could be tuned by varying the amount of surfactant in the deposition mixtures or by adjusting the humidity during the drying process. Note that this behavior was not observed if CTAB was used as the structure-directing agent; this might be due to the fact that CTAB is an ionic template and therefore interacts differently with the silica precursors and the AAM surface. The corresponding SAXS patterns of the mesophase structures that were prepared in the channels of the AAMs with deposition solutions that contained increasing amounts of template and synthesized at different humidities are shown in Figure 4b and c, respectively. All the patterns can be described as superpositions of the patterns typical for the structures that exhibit a columnar orientation (Figure 3a) and those with the circular mesophase structure (Figure 3b). This implies that the in-plane reflections will be preserved in any case, whereas both out-of-plane reflections should appear with decreased intensity in the case of mixed structures. The intensity ratios (10)/(01) for the P123- and Brij56-templated silica material in the AAMs are shown in Table 2. It is striking that by increasing the concentration of surfactant in the deposition mixtures and by carrying out the synthesis at high humidity, a drastic shift in population towards the columnar mesostructures results. It was observed in both cases that the drying of the composite material, which usually took between three to five hours, takes longer than at lower humidity or with a lower concentration of surfactant. We therefore suggest that there is a small energy difference between both orientations and that with a longer reaction time the reaction is driven towards the thermodynamically more stable state which results in the vertical, columnar mesopore alignment.

Table 2: Summary of SAXS data of block-copolymer-templated mesoporous channel systems.

Sample	Surfactant/silica molar ratio	Relative integrated intensities of diffraction spots, (10)/(01)[a]			*d* spacings[b]
		60% humidity	40% humidity	20% humidity	
B1–B3	Brij56/Si = 0.133	0.5	0.75	0.96	6.2 (B1) 6.0 (B2) 5.8 (B3)
C1–C3	Brij56/Si = 0.265	0	0.03	0.3	6.4
D1, D2	P123/Si = 0.013	1.1	1.0	[c]	11.0
E1, E2	P123/Si = 0.017	0.03	0.3	[c]	11.5

[a] The intensity of the reflections was normalized to the intensity of the primary beam after the semitransparent beam stop. [b] The *d* spacings were calculated from the position of the diffraction spots according to $q = 2\pi/d$. [c] No structure detected.

When P123 was used as structure-directing agent, the reflections corresponding to the circular mesopore orientation did not completely vanish. This effect may be related to the larger pore diameter of these structures, which implies that the ratio of the diameter of the mesopore to the diameter of the AAM channel differs significantly from the analogous ratios for samples synthesized with CTAB or Brij56. Thus the curvature of the AAM channel wall may drive the micelles towards the circular orientation.

The corresponding plan-view TEM images (Figure 5b and c for the Brij56- and P123-templated structures, respectively) show the circular orientation as well as highly ordered hexagonal structures arising from the columnar mesopore orientation that are present in different relative populations. The cross-sectional images shown in Figure 5d (P123-templated structure E1) illustrate the predominantly columnar alignment of the embedded mesoporous channels within the AAM channels, as well as the hexagonal structure that becomes visible when the cross-section of the circular mesopore orientation is viewed. The plan-view TEM images also show the coexistence of the circular and columnar mesopores in different channels of the AAMs or, in some cases, "twinned" structures that show both configurations.

The embedded silica–surfactant nanocomposite mesophases obtained here differ significantly from those reported previously for confined polymer systems[18] in that the mesostructures discussed in the present study form a rigid silica framework upon removal of the template, to leave solid supports with ordered porosity that can, for example, offer a matrix for the guided growth of a variety of conductive materials. Recent research on the 1D confinement of conductive nanostructures has shown that extended control over the morphology and size of such structures is important for their potential application in integrated electronic circuits.[19,20]

To summarize, this study of the 1D confinement of silica–surfactant composites in the vertical channels of anodic alumina membranes showed that new, mesoscopic structures with intriguing arrangements of the mesoporous channels are possible. We demonstrated that three of the most commonly used structure-directing agents (CTAB, P123, and Brij56) can be employed for the synthesis of hexagonally ordered mesoporous silica embedded in AAM channels. The formation of both circular and columnar phases can take place, and with the non-ionic surfactants the occurrence of these phases can be tuned by changing the concentration of the surfactant and the humidity in the adjacent gas phase. The structural features of the CTAB-, Brij56-, and P123-templated mesoporous filaments in the AAMs will allow the fast and effective inclusion of a variety of interesting 1D nanostructures, which range from metallic nanowires, semiconductor nanoparticles and nanowires, to carbon nanotubes.

Experimental Section

Preparation of the samples: The deposition mixtures were prepared by applying a two-step synthesis procedure: First, tetraethyl orthosilicate (Aldrich; 2.08 g, 0.01 mol) was mixed with 0.2 M HCl (3 g), H_2O (1.8 g), and EtOH (5 mL), and the mixture was heated at 60 °C for 1 h to carry out acid-catalyzed hydrolysis–condensation of the silica precursor. For the preparation of CTAB-containing deposition mixtures, this solution was mixed with CTAB (0.644 g, 1.77 mmol for sample CTAB1; or 0.947 g, 2.6 mmol for CTAB2) dissolved in EtOH (10 mL). The Brij56-containing samples were prepared using Brij56 (0.906 g, 1.33 mmol dissolved in ethanol (15 mL) or 1.81 g, 2.65 mmol dissolved in ethanol (30 mL) for samples B1–B3 and C1–C3, respectively). For the preparation of the P123-containing solutions, the prehydrolyzed silica was mixed with 5 wt % solutions of P123 in ethanol: 15 mL (0.13 mmol P123 for sample D1–D3) or 20 mL (0.17 mmol P123 for sample E1–E3). The AAMs (47 mm, Anodisc, Whatman) with average pore diameters of 120–200 nm and a thickness of approximately 60 μm were soaked with the prepared mixtures of the precursor by distributing 0.75 mL of the solutions over the whole membrane surface. After 3–5 h at room temperature and under controlled humidity, the membrane appeared dry and homogeneously filled with the mixture.

Characterization of the embedded silica mesostructures: GI-SAXS measurements were performed with a SAXSess small-angle X-ray scattering system by Anton Paar after alignment of the X-ray beam with the surface of the sample as shown in Figure 3. The incident beam was shadowed with a circular beam stop, and the signal was recorded on image plates after collecting the pattern for 1 h. The TEM images were obtained with a JEOL 2010 transmission electron microscope operating at 200 kV. Samples for electron microscopy were prepared by the following method: 1) the alumina matrix was dissolved in phosphoric acid to release the embedded mesoporous silica; 2) plan views and cross-sections were prepared by dimple grinding followed by Ar ion polishing. The elemental composition and surface morphology of the samples were determined by SEM using a JEOL JSM 6500F field emission scanning electron microscope equipped with an Oxford EDX detector.

Received: September 16, 2005
Published online: January 3, 2006

Keywords: host–guest systems · membranes · mesoporous materials · surfactants · template synthesis

[1] A. P. Wight, M. E. Davis, *Chem. Rev.* **2002**, *102*, 3589.
[2] B. J. Scott, G. Wirnsberger, G. D. Stucky, *Chem. Mater.* **2001**, *13*, 3140.
[3] C. J. Brinker, Y. Lu, A. Sellinger, H. Fan, *Adv. Mater.* **1999**, *11*, 579.
[4] D. Grosso, F. Babonneau, P.-A. Albouy, H. Amenitsch, A. R. Balkenende, A. Brunet-Bruneau, J. Rivory, *Chem. Mater.* **2002**, *14*, 931.
[5] M. Klotz, P.-A. Albouy, A. Ayral, C. Menager, D. Grosso, A. van der Lee, V. Cabuil, F. Babonneau, C. Guizard, *Chem. Mater.* **2000**, *12*, 1721.
[6] G. Kickelbick, *Small* **2005**, *1*, 168 – 170.
[7] Z. Yang, Z. Niu, X. Cao, Z. Yang, Y. Lu, Z. Hu, C. C. Han, *Angew. Chem.* **2003**, *115*, 4333 – 4335; *Angew. Chem. Int. Ed.* **2003**, *42*, 4201 – 4203.
[8] F. Marlow, I. Leike, C. Weidenthaler, C. W. Lehmann, U. Wilczok, *Adv. Mater.* **2001**, *13*, 307 – 310.
[9] F. Kleitz, F. Marlow, G. D. Stucky, F. Schüth, *Chem. Mater.* **2001**, *13*, 3587.
[10] A. Yamaguchi, F. Uejo, T. Yoda, T. Uchida, Y. Tanamura, T. Yamashita, N. Teramae, *Nat. Mater.* **2004**, *3*, 337.
[11] Y. Wu, G. Cheng, K. Katsov, S. W. Sides, J. Wang, J. Tang, G. H. Fredrickson, M. Moskovits, G. D. Stucky, *Nat. Mater.* **2004**, *3*, 816.
[12] Q. Lu, F. Gao, S. Komarneni, T. E. Mallouk, *J. Am. Chem. Soc.* **2004**, *126*, 8650.
[13] D. Wang, R. Kou, Z. Yang, J. He, Z. Yang, Y. Lu, *Chem. Commun.* **2005**, 166.
[14] B. Yao, D. Fleming, M. A. Morris, S. E. Lawrence, *Chem. Mater.* **2004**, *16*, 4851.
[15] K. Jin, B. Yao, N. Wang, *Chem. Phys. Lett.* **2005**, *409*, 172.
[16] A. Y. Ku, S. T. Taylor, S. M. Loureiro, *J. Am. Chem. Soc.* **2005**, *127*, 6934.
[17] A. Monnier, F. Schüth, Q. Huo, D. Kumar, D. Margolese, R. S. Maxwell, G. D. Stucky, M. Krishnamurty, P. Petroff, A. Firouzi, M. Janicke, B. F. Chmelka, *Science*, **1993**, *261*, 1299.
[18] J. Y. Cheng, A. M. Mayes, C. A. Ross, *Nat. Mater.* **2004**, *3*, 823.
[19] M. L. Cohen, *Mater. Sci. Eng. C* **2001**, *15*, 1.
[20] Y. Xia, P. Yang, Y. Sun, Y. Wu, B. Mayers, B. Gates, Y. Yin, F. Kim, H. Yan, *Adv. Mater.* **2003**, *15*, 353.

